

Error from Delay Drift in Terahertz Attenuated Total Reflection Spectroscopy

A. Soltani · T. Probst · S. F. Busch ·
M. Schwerdtfeger · E. Castro-Camus · M. Koch

Received: 14 November 2013 / Accepted: 16 January 2014 /
Published online: 5 March 2014
© Springer Science+Business Media New York 2014

Abstract In this article we discuss the influence of temporal stability on the value obtained for dielectric properties of materials measured by terahertz time-domain spectroscopy with particular emphasis on attenuated total reflection. The stability of three different terahertz attenuated total reflection spectroscopy systems is carefully characterized. The formalism for the complex refractive index extraction is presented and the effect of delay errors is calculated numerically. We found that good thermal stability of the terahertz system helps to minimize delay fluctuations and therefore the uncertainty of the resulting complex refractive index.

Keywords Attenuated total reflection · Delay shift · Uncertainty · Error

The field of terahertz spectroscopy has seen enormous progress over the last three decades, but very particularly over the last ten years [1]. Among the most important advances is the establishment of the technique known as terahertz time-domain spectroscopy (THz-TDS) [2]. Owing to its extraordinary signal to noise performance TDS is probably the most widely used and powerful spectroscopic technique for the far infrared band [3]. TDS has opened the possibility to study a wealth of systems in the band between microwaves and infrared (30 GHz to 10 THz or 30 μm and 10 mm) that include crystalline solids [4, 5], liquids [6], gases [7] and many other systems

A. Soltani · T. Probst · S. F. Busch · M. Schwerdtfeger · M. Koch
Faculty of Physics and Material Sciences Center, Philipps-Universität Marburg,
Renthof 5, 35032 Marburg, Germany

E. Castro-Camus (✉)
Centro de Investigaciones en Óptica A.C.,
Loma del Bosque 115, Lomas del Campestre, León, Guanajuato 37150, México
e-mail: enrique@cio.mx

[8–10]. Furthermore, enormous progress has been achieved in the development of filters [11], modulators [12] and other components for this spectral band.

Time-domain spectroscopy is based on the use of femtosecond near-infrared pulses to generate single cycle electromagnetic transients of radiation either by ultra-fast charge separation [13–15], or by optical rectification in a non-linear crystal [16]. Unlike in traditional optics where radiation is detected either by bolometric or photon-counting devices THz-TDS uses a fraction of the same femtosecond pulse mentioned earlier to gate a detector that is used to map the temporal waveform of the electric field. This makes TDS immune to thermal background noise. However, time-domain setups are not noise or uncertainty free, this has been discussed previously in the literature [17, 18].

A system of study that has attracted particular interest within the terahertz community is water. The strong interaction of water with terahertz radiation is caused by its collective dynamics [19, 20], which at its time, plays a key role in the way it interacts with proteins and other biomolecules [21]. Therefore the study of proteins in aqueous solution using terahertz radiation is of enormous importance to understand their interaction and function [22–28]. Yet, these studies have proven challenging given that transmission of terahertz through water is relatively low. Therefore schemes to obtain the dielectric properties of water itself and aqueous solutions in reflection geometries have been proposed [29, 30]. Among those schemes, attenuated total reflection (ATR) is probably the most widely used [31–34].

In this article we evaluate the effect of delay drift between the THz-generation and detector-gate pulses. These drift can cause significant errors for transmission spectroscopy of thin films [35], but very particularly for reflection spectroscopic techniques such as ATR. Therefore we discuss how these errors propagate through the data processing and their impact on the final refractive index and absorption coefficient measured by ATR. We, additionally, present experimental evidence that this technique is particularly susceptible to small fluctuations on the relative delay used in TDS setups. We also evaluate the magnitude of such fluctuations with three different TDS systems and conclude that the fluctuations in the mutual pulse delay are mostly related to temperature changes and not necessarily related to mechanical stage imperfections.

1 Fluctuations of ATR for Different Spectroscopy Systems

Three different THz spectrometers were used for this report.

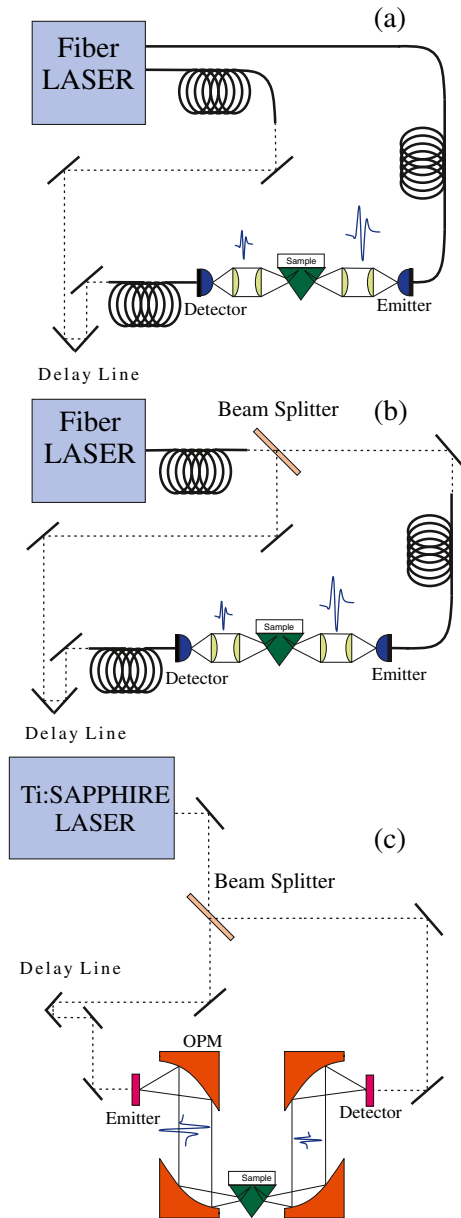
- System A (Fiber setup): Is a THz-TDS (shown in Fig. 1a) setup based on an Er:Fiber laser which provides 90 fs pulses with a central wavelength of 1560 nm at a repetition rate of 100 MHz with an average power of ~ 80 mW. These pulses are divided inside the laser and coupled out using two fiber ports. After propagating through 6 m of fiber, the pulses of one of the arms are coupled out into free-space and delayed using a computer controlled mechanical stage. This beam is coupled back into a 1.05 m fiber that guides it to an LT-InGaAs/InAlAs stripline photoconductive emitter antenna with a gap between contacts of 25 μm

- biased by 20 V. The generated terahertz radiation is collimated and focused by a pair of polyethylene lenses, it subsequently propagates through a HR-FZ Silicon prism (as shown on Fig. 1a). Another pair of polyethylene lenses is used to collect and focus the transmitted THz radiation onto a photoconductive detector. The pulses from the second port of the laser are guided through 7.05 m of fiber onto a 10 μm dipole photoconductive detector fabricated on LT-InGaAs/InAlAs.
- System B (Semi fiber setup): Is a THz-TDS (shown in Fig. 1b) based on the same laser as described in system A. In this system only one port of the laser was used supplying ~ 50 mW of average power. The laser is guided through 6 m of optical fiber. This beam is coupled out into the free space and using a polarizing beam splitter cube (1200–1600 nm) the laser pulses are divided into two parts. The first part is delayed using a computer controlled mechanical stage. This beam is coupled back into a 1.05 m fiber that guides it to an LT-InGaAs/InAlAs stripline photoconductive emitter antenna with a gap between contacts of 25 μm biased by 20 V. After generation the THz transients are collimated and focused by a pair of polyethylene lenses, subsequently the THz radiation propagates through a HR-FZ Silicon prism (as shown on Fig. 1b). Another pair of polyethylene lenses is used to collect and focus the transmitted THz radiation onto a photoconductive detector. The second part of the femtosecond pulses from the beam is guided through a 1.05 m of optical fiber onto a LT-InGaAs/InAlAs detector.
 - System C (Free space setup): Is a standard THz time-domain system is based on a Ti:Sapphire femtosecond laser which provides 70 fs pulses with a central wavelength of 780 nm at a repetition rate of 80 MHz with an average power of ~ 100 mW. The laser pulses are divided using a beam splitter. The first part is delayed using a computer controlled mechanical stage. This beam is used to excite a SI-GaAs stripline photoconductive emitter antenna with a gap between contacts of 10 μm biased by 20 V. The produced terahertz radiation is collimated and focused by a pair of off-axis parabolic mirrors. It subsequently propagates through a HR-FZ Silicon prism (as shown in Fig. 1c). Another pair of off-axis parabolic mirrors is used to collect and focus the transmitted THz radiation onto a photoconductive detector antenna. The second part of the laser is used to gate a 5 μm dipole photoconductive detector fabricated on LT-GaAs.

All three systems used the same computer controlled delay line (PI: M-521.DG) and the the same data acquisition parameters via an SR830 lock-in amplifier. All fibers shown in Fig. 1 are polarizations maintaining fibers.

In Fig. 2a and b we show the refractive index and absorption coefficient of water extracted from ten consecutive measurements performed with a fully fiber coupled ATR-TDS system (System A). Note that the curves on both panels show very large differences, ~ 0.3 for refractive index and ~ 60 cm^{-1} at 1 THz. This enormous statistical dispersion (~ 20 %) is unacceptable for reliable spectroscopy in research labs or for practical application in industry. In Fig. 2c and d ten additional measurements of the refractive index and absorption coefficient are presented. In this case

Fig. 1 (Color online) **a** Fiber coupled THz-TDS setup. **b** Semi-fiber coupled THz-TDS setup. **c** Free-space THz-TDS setup



the measurements were performed in a spectrometer in which most of the optical paths happen through free-space and only the last meter before reaching the emitter or detector are fiber guided (System B). In this case the measurements show less statistical dispersion, at 1 THz the measurements vary by ~ 0.03 for refractive index and $\sim 12 \text{ cm}^{-1}$ for absorption coefficient.

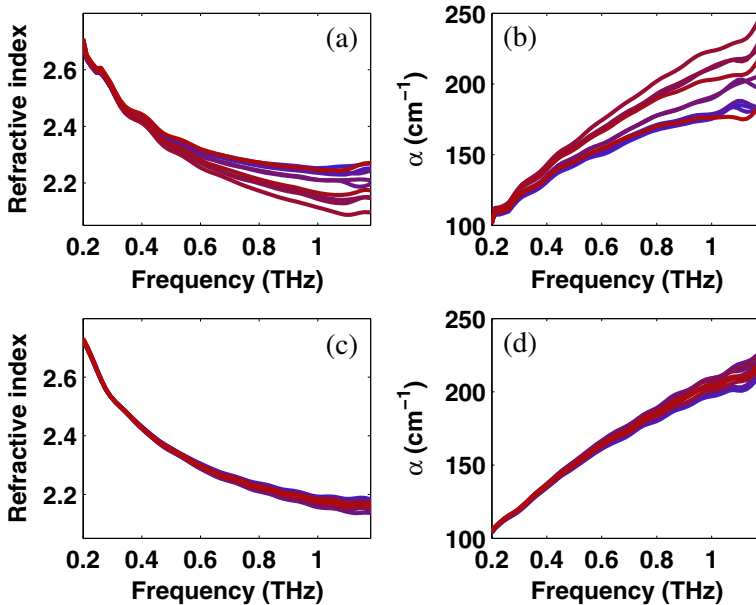


Fig. 2 (Color online) The refractive indices (a) and absorption coefficients (b) obtained from ten consecutive measurements using a TDS system A (fiber). (c) and (d) are analogous measurements using TDS system B (semi-fiber)

2 Delay Stability

In order to find out what the difference between these two systems is, we acquired 150 terahertz waveforms with each over the course of several three hours in the absence of sample. In addition we used system C, which is a fully free-space system. In Fig. 3a, b and c the 150 waveforms are plotted. The difference is more or less evident. The fully fiber coupled system shows enormous delay drifts between scans, while the semi-fiber and free-space systems show almost perfect overlap for all their pulses. In order to quantify this drift, the absolute value of the deviation of the zero-field crossing point after the main peak for each scan is shown in Fig. 3d. Notice that this is presented in logarithmic scale. The standard deviation of the fiber system zero-crossing position is of the order of 140 fs, while the semi-fiber and free-space systems presents a drift of 6 fs and 2 fs respectively. All of these measurements were carried out in temperature controlled laboratories. Continuous recording of the temperature on the optical bench area of each laboratory demonstrates that the temperature was very stable (< 0.08 °C standard deviation).

From the previous measurements it is clear that the delay drift of the fiber system causes significant errors on the ATR measurements. In order to have a more quantitative feeling for the effect that the drift has on the measured refractive index and absorption coefficient we decided to model the effect of rigid shifts on the sample pulse with respect to de reference pulse. Before presenting such results, we

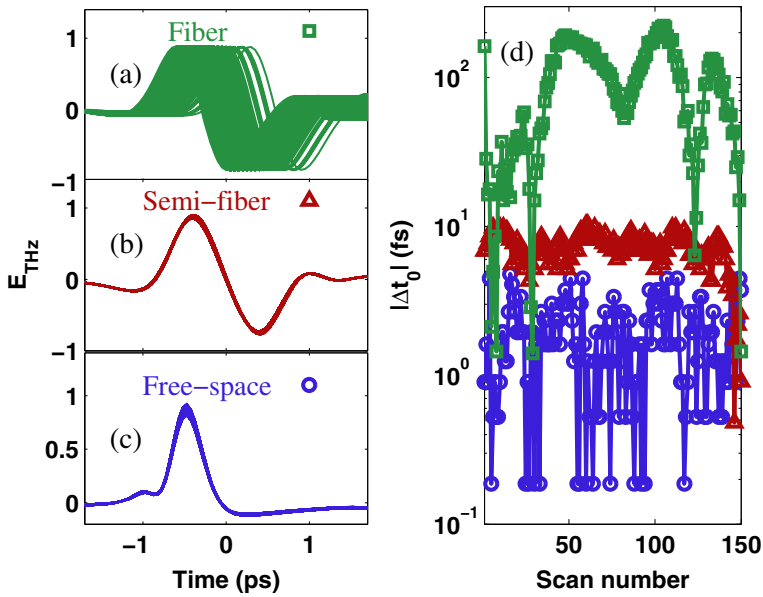


Fig. 3 (Color online) One hundred and fifty consecutive time-domain scans using a fiber (a), semi-fiber (b) and free-space (c) system. In (d) the deviation zero-crossing from the average position for the pulses from the 150 pulses recorded using a fiber (squares), semi-fiber (triangles) and free-space (circles) system

would like to go through the formalism to extract the complex refractive index from the ATR measurements.

3 ATR Data Processing and Uncertainty

The complex transfer function for the system is the ratio between the Fourier transforms of the terahertz pulses recorded in the presence and absence of sample on top of the prism. Given that the trajectory of the terahertz radiation is the same for the reference and the sample pulses, the transfer function can be written in terms of the reflection coefficient (for p-polarization) at the prism-sample $r_{Si,sam}$ and the prism-air $r_{Si,air}$ interface

$$T(\omega) = \frac{E_{sam}(\omega)}{E_{ref}(\omega)} = \frac{r_{Si,sam}(\omega)}{r_{Si,air}(\omega)}. \tag{1}$$

The reflection coefficient between any two media (i, j) is given by

$$r_{i,j}(\omega) = \frac{\tilde{n}_i(\omega)C_{i,j}(\omega) - \tilde{n}_j(\omega) \cos \theta_i}{\tilde{n}_i(\omega)C_{i,j}(\omega) + \tilde{n}_j(\omega) \cos \theta_i}, \tag{2}$$

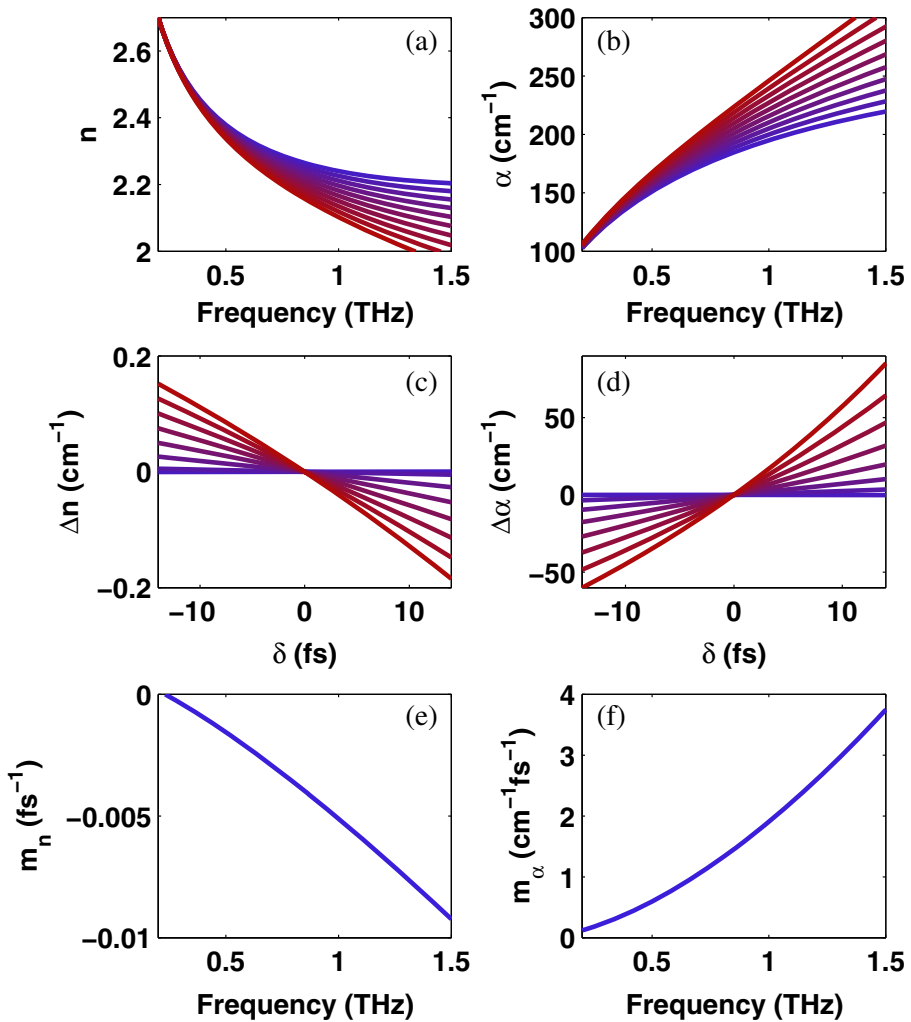


Fig. 4 (Color online) Refractive index (a) and absorption coefficient (b) for water calculated using $E_{\text{sam}}(t - \delta)$ with a controlled delay shift $-15 \text{ fs} < \delta < 15 \text{ fs}$, the curves show how the introduction of a rigid delay shift introduces errors on the final dielectric properties. On panels (c) and (d) the deviation from the correct value is show as function of δ for various frequencies between 0 and 1.5 THz. On panels (e) and (f) the slope of the lines in (c) and (d) is shown as function of frequency, these curves give a measure of how susceptible the refractive index and absorption coefficient are fluctuations in the delay

where \tilde{n}_i is the complex refractive index of the i -th medium and

$$C_{i,j} = \sqrt{1 - \frac{\tilde{n}_i^2(\omega)}{\tilde{n}_j^2(\omega)} \sin^2 \theta_i}. \quad (3)$$

From these equations it is clear that if both, the refractive index of air and silicon (prism) are known, and the transfer function can be obtained from the experiment, after algebraic manipulation, it is possible to obtain the refractive index of the sample

$$\tilde{n}_{\text{sam}}(\omega) = X(\omega)\tilde{n}_{\text{Si}}(\omega), \tag{4}$$

where

$$X(\omega) = \sqrt{\frac{-A(\omega)^2 \pm \sqrt{A(\omega)^4 - 4 \sin^2 \theta_i}}{2}}, \tag{5}$$

with

$$A(\omega) = \frac{1 - r_{\text{Si,sam}}(\omega)}{1 + r_{\text{Si,sam}}(\omega)}, \tag{6}$$

which at its time is obtained from the experimental transfer function using Eq. 1. In Eq. 5 both solutions are mathematically correct, yet only the positive sign of the square root is kept owing to the fact that the imaginary part of the dielectric function has to be positive in order to comply with causality.

In order to quantify the error produced on n and α by a rigid delay shift in the time domain, such as the fluctuations observed in Fig. 3 we decided to take a numerical approach. In Fig. 4a and b the refractive index calculated for artificial delays introduced numerically in 1 fs steps. In Fig. 4c and d the deviation from the original measurement as function of the introduced delay is shown for various frequencies. Notice that all these curves are linear, therefore, the slope of such lines will give a measure of how susceptible the refractive index and absorption coefficient to delay fluctuations is each for frequency. The slope for these lines as function of frequency is shown in Fig. 4e and f. From the plots it is clear the dielectric properties for higher frequencies (shorter wavelengths) will be more susceptible to fluctuations, which is not only reasonable, but also consistent with the observations presented in Fig. 2. The curves on Fig. 4e and f give a quantitative measure of how susceptible the refractive index and absorption coefficient are to delay fluctuations as function of frequency.

4 Final Remarks

The effect of fluctuations in the delay between the sample and reference pulses induced by delay drift of the system itself can have a very significant effect on ATR measurements. This is also true for measurements of dielectric properties by other forms of time-domain reflection spectroscopy and even for transmission spectroscopy in the case of thin samples. We found that the delay fluctuations are more significant in fiber coupled systems. We also found that the temperature stability of the laboratory is critical in order minimize these drifts.

The advantages of fiber coupled systems for “real-world” applications are well known. These systems are far more stable, robust and flexible, therefore the implementation of reflection or transmission (in the case of thin samples) time-domain spectroscopy based on systems of this kind will require further engineering in order to obtain accurate results. Users of these technologies are encouraged to perform a careful characterization of the delay drift of their systems in order to determine if the accuracy they can achieve is good enough for their particular application.

Acknowledgments We gratefully acknowledge funding by the German Federal Ministry of Economics and Technology through the project 61308462 and CONAcYt through grant number 131931. Amin Soltani acknowledges funding by the German Academic Exchange Service.

References

1. M Tonouchi. Cutting-edge terahertz technology. *Nat. Photon.*, 1:97–105, 2007.
2. P U Jepsen, D G Cooke, and M Koch. Terahertz spectroscopy and imaging - modern techniques and applications. *Laser Photon. Rev.*, 5:124–166, 2011.
3. C A Schmuttenmaer. Exploring dynamics in the far-infrared with terahertz spectroscopy. *Chem. Rev.*, 104:1759–1779, 2004.
4. H Zhan, V Astley, M Hvasta, J A Deibel, D M Mittleman, and Y Lim. The metal-insulator transition in VO_2 studied using terahertz apertureless near-field microscopy. *Appl. Phys. Lett.*, 91:162110, 2007.
5. James Lloyd-Hughes and Tae-In Jeon. A review of the terahertz conductivity of bulk and nano-materials. *Journal of Infrared, Millimeter, and Terahertz Waves*, 33(9):871–925, 2012.
6. John F Federici. Review of moisture and liquid detection and mapping using terahertz imaging. *Journal of Infrared, Millimeter, and Terahertz Waves*, 33(2):97–126, 2012.
7. H W Hübers, S G Pavlov, H Richter, A D Semenov, L Mahler, A Tredicucci, H E Beere, and D A Ritchie. High-resolution gas phase spectroscopy with a distributed feedback terahertz quantum cascade laser. *Appl. Phys. Lett.*, 89:061115, 2006.
8. Kaori Fukunaga, Yuichi Ogawa, Shin'ichiro Hayashi, and Iwao Hosako. Terahertz spectroscopy for art conservation. *IEICE Electronics Express*, 4(8):258–263, 2007.
9. R Gente, N Born, N Voß, W Sannemann, J Léon, M Koch, and E Castro-Camus. Determination of leaf water content from terahertz time-domain spectroscopic data. *Journal of Infrared, Millimeter and Terahertz Waves*, 34(3-4):316–323, 2013.
10. M Schwerdtfeger, E Castro-Camus, K Krügener, W Viöl, and M Koch. Beating the wavelength limit: three-dimensional imaging of buried subwavelength fractures in sculpture and construction materials by terahertz time-domain reflection spectroscopy. *Applied Optics*, 52(3):375–380, 2013.
11. N Vieweg, N Born, I Al-Naib, and M Koch. Electrically tunable terahertz notch filters. *Journal of Infrared, Millimeter, and Terahertz Waves*, 33(3):327–332, 2012.
12. Marco Rahm, Jiu-Sheng Li, and Willie J Padilla. Thz wave modulators: a brief review on different modulation techniques. *Journal of Infrared, Millimeter, and Terahertz Waves*, 34(1):1–27, 2013.
13. CW Berry, N Wang, MR Hashemi, M Unlu, and M Jarrahi. Significant performance enhancement in photoconductive terahertz optoelectronics by incorporating plasmonic contact electrodes. *Nature communications*, 4:1622, 2013.
14. M B Johnston, D M Whittaker, A Corchia, A G Davies, and E H Linfield. Simulation of terahertz generation at semiconductor surfaces. *Phys. Rev. B*, 65:165301, 2002.
15. G Klatt, F Hilser, W Qiao, M Beck, R Gebis, A Bartels, K Huska, U Lemmer, G Bastian, M B Johnston, M Fischer, J Faist, and T Dekorsy. Terahertz emission from lateral photo-Dember currents. *Opt. Express*, 18:4939–4947, 2010.
16. A Nahata, A S Welington, and T F Heinz. A wideband coherent terahertz spectroscopy system using optical rectification and electro-optic sampling. *Appl. Phys. Lett.*, 69:2321, 1996.
17. L Duvaillaret, F Garet, and J-L Coutaz. Influence of noise on the characterization of materials by terahertz time-domain spectroscopy. *J. Opt. Soc. Am. B-Opt. Phys.*, 17:452–461, 2000.
18. W Withayachumnankul, B M Fischer, H Y Lin, and D Abbott. Uncertainty in terahertz time-domain spectroscopy measurement. *J. Opt. Soc. Am. B-Opt. Phys.*, 25:1059–1072, 2008.
19. J Xu, K W Plaxco, and S J Allen. Absorption spectra of liquid water and aqueous buffers between 0.3 and 3.72 thz. *J. Chem. Phys.*, 124:036101, 2006.
20. M Heyden, J A Sun, S Funkner, G Mathias, H Forbert, M Havenith, and D Marx. Dissecting the thz spectrum of liquid water from first principles via correlations in time and space. *Proc. Natl. Acad. Sci. U. S. A.*, 107:12068–12073, 2010.
21. Benjamin Born and Martina Havenith. Terahertz dance of proteins and sugars with water. *Journal of Infrared, Millimeter, and Terahertz Waves*, 30(12):1245–1254, 2009.

22. J Xu, K W Plaxco, and S J Allen. Probing the collective vibrational dynamics of a protein in liquid water by terahertz absorption spectroscopy. *Protein Sci.*, 15:1175–1181, 2006.
23. S Ebbinghaus, S J Kim, M Heyden, X Yu, U Heugen, M Gruebele, D M Leitner, and M Havenith. An extended dynamical hydration shell around proteins. *Proc. Natl. Acad. Sci. U. S. A.*, 104:20749–20752, 2007.
24. U Heugen, G Schwaab, E Brundermann, M Heyden, X Yu, D M Leitner, and M Havenith. Solute-induced retardation of water dynamics probed directly by terahertz spectroscopy. *Proc. Natl. Acad. Sci. U. S. A.*, 103:12301, 2006.
25. J Xu, K W Plaxco, and S J Allen. Collective dynamics of lysozyme in water: terahertz absorption spectroscopy and comparison with theory. *J. Phys. Chem. B*, 110:24255–24259, 2006.
26. Seung Joong Kim, Benjamin Born, Martina Havenith, and Martin Gruebele. Real-time detection of protein-water dynamics upon protein folding by terahertz absorption spectroscopy. *Angewandte Chemie International Edition*, 47(34):6486–6489, 2008.
27. E Castro-Camus and M B Johnston. Conformational changes of photoactive yellow protein monitored by terahertz spectroscopy. *Chem. Phys. Lett.*, 455:289–292, 2008.
28. Robert J Falconer and Andrea G Markelz. Terahertz spectroscopic analysis of peptides and proteins. *Journal of Infrared, Millimeter, and Terahertz Waves*, 33(10):973–988, 2012.
29. C Ronne, L Thrane, P O Astrand, A Wallqvist, K V Mikkelsen, and S R Keiding. Investigation of the temperature dependence of dielectric relaxation in liquid water by thz reflection spectroscopy and molecular dynamics simulation. *J. Chem. Phys.*, 107:5319, 1997.
30. L Thrane, RH Jacobsen, P Uhd Jepsen, and SR Keiding. Thz reflection spectroscopy of liquid water. *Chemical Physics Letters*, 240(4):330–333, 1995.
31. Atsushi Nakanishi, Yoichi Kawada, Takashi Yasuda, Koichiro Akiyama, and Hironori Takahashi. Terahertz time domain attenuated total reflection spectroscopy with an integrated prism system. *Rev. Sci. Instrum.*, 83:033103, 2012.
32. Masaya Nagai, Hiroyuki Yada, Takashi Arikawa, and Koichiro Tanaka. Terahertz time-domain attenuated total reflection spectroscopy in water and biological solution. *International journal of infrared and millimeter waves*, 27(4):505–515, 2006.
33. Hideki Hirori, Kumiko Yamashita, Masaya Nagai, and Koichiro Tanaka. Attenuated total reflection spectroscopy in time domain using terahertz coherent pulses. *Japanese journal of applied physics*, 43:1287, 2004.
34. D Y K Ko and J R Sambles. Scattering matrix-method for propagation of radiation in stratified media - attenuated total reflection studies of liquid-crystals. *J. Opt. Soc. Am. A-Opt. Image Sci. Vis.*, 5:1863–1866, 1988.
35. John F O'Hara, Withawat Withayachumnankul, and Ibraheem Al-Naib. A review on thin-film sensing with terahertz waves. *Journal of Infrared, Millimeter, and Terahertz Waves*, 33(3):245–291, 2012.